International Journal of Electrical, Electronic and Communication Sciences
ISSN: 2517-9438
Vol:12, No:12, 2018

An Investigation of a Three-Dimensional Constitutive Model of Gas Diffusion Layers in Polymer Electrolyte Membrane Fuel Cells

Yanqin Chen, Chao Jiang, Chongdu Cho

***Abstract*—**This research presents the three-dimensional mechanical characteristics of a commercial gas diffusion layer by experiment and simulation results. Although the mechanical performance of gas diffusion layers has attracted much attention, its reliability and accuracy are still a major challenge. With the help of simulation analysis methods, it is beneficial to the gas diffusion layer's extensive commercial development and the overall stress analysis of proton electrolyte membrane fuel cells during its pre-production design period. Therefore, in this paper, a three-dimensional constitutive model of a commercial gas diffusion layer, including its material stiffness matrix parameters, is developed and coded, in the user-defined material model of a commercial finite element method software for simulation. Then, the model is validated by comparing experimental results as well as simulation outcomes. As a result, both the experimental data and simulation results show a good agreement with each other, with high accuracy.

***Keywords*—**Gas diffusion layer, proton electrolyte membrane fuel cell, stiffness matrix, three-dimensional mechanical characteristics, user-defined material model.

I. Introduction

POLYMER Electrolyte Membrane Fuel Cells (PEMFCs) [1]-[3] are extensively and commercially applied in transportation, aviation, residential power generation, and portable devices, with some excellent benefits including low emission, low weight, high current density, fast start-ups and long stack life, etc. A PEMFC is mechanically sandwiched as a stack with bipolar plates (BPPs) and a membrane electrode assembly (MEA). The MEA is composed of a polymer electrode membrane (PEM), two catalyst layers (CLs) and two gas diffusion layers (GDLs) [4]. In a fuel cell unit, the GDL is stacked, between BPPs with flow channels and catalyst layers, under the clamping pressure of 0.5-2.5 MPa [5], [6]. The clamping pressure could result in inhomogeneous stress distributions in the GDL due to the ribbed structure of flow channels on BPPs [7]. The mechanical properties of GDL, as a core component of PEMFCs, have a great impact on the overall performance of fuel cells.

Recently, the investigation of GDLs has sprung up and especially focused on how its characteristics are influenced during fabrication, operation, degradation, and assembly process [8]-[10]. Meanwhile, GDLs' characterization techniques, components, key properties (such as structure, porosity, hydrophobicity, permeability, transport properties, and surface morphology, etc.), microstructure modeling, and durability, are widely investigated and reviewed [11]-[17]. Dhanushkodi et al. [18] reported that the physical and mechanical properties of GDLs depend on the carbon-carbon composite interaction and fabrication process. In addition to these, they indicated that GDLs' mechanical degradation behavior relies on fiber length and load transfer directions. Gigos et al. [19] presented the GDL's experimental investigation and developed its analytical model by considering the periodical compression loads running during the PEMFC's operation. It was proved that there is a good agreement between the experimental data and simulation results from the analytical model. Most literature concentrated on the study of GDLs' compression behavior [20]-[24]. Unfortunately, GDLs were simply considered as isotropic materials [25]. However, GDLs show obvious anisotropic properties due to the orientation of carbon fibers in it [26]-[28]. Additionally, GDLs withstand complicated and inhomogeneous clamping loads from all directions in PEMFCs [29]. Thus, the 3D characterization analysis of GDLs should be achieved, which can precisely predict its deformation, improve the reliability of its mechanical performance, and optimize the assembly pressure.

Convincing assessment and prediction of GDLs' mechanical performance should be done by combing experimental characterization methods as well as model simulation analysis. This research presented the 3D mechanical characterization of a commercial GDL by experimental results and simulation outcomes. Significantly, a comprehensive finite element analysis model of the GDL was developed. Subsequently, the model was implemented in the UMAT part of ABAQUS by coding, for its mechanical characteristics simulation results. Finally, the simulation results and experimental data were compared for the model verification.

II. Model Descriptions

Based on the GDL's assembly configurations in a real fuel cell stack, GDLs are subjected loads from all directions. Thus, we defined the GDL's dimensions as shown in Fig. 1. The GDL's compressive behavior in Z (thickness) direction, tensile performance in X and Y directions (in-plane) and shear characteristics in ZX and ZY planes were explored at room condition, respectively. In this paper, a commercial GDL (Type: JNT 30-A1, from JNT Group company, in Hwasung-si,

Yanqin Chen and Chao Jiang are with the Department of Mechanical Engineering, Inha University, Incheon 22212, South Korea (e-mail: chenyanqin2008@outlook.com, chiaojiang@outlook.com).

Chongdu Cho is with the Department of Mechanical Engineering, Inha University, Incheon 22212, South Korea (corresponding author, phone: 82-32-860-7321; fax: 82-32-872-7322; e-mail: cdcho@ inha.ac.kr).

South Korea) was employed as specimens for all the tests.

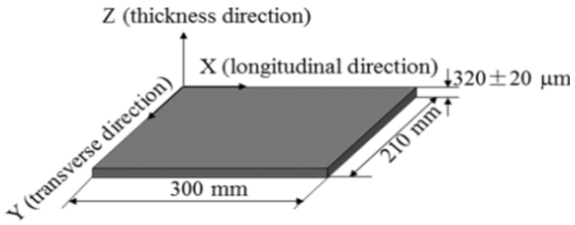

Fig. 1 Dimension definition of the commercial GDL paper sheet

A. Compression Numerical Model

Norouzifard and Bahrami [30] developed a compact compressive analytical model of a GDL, including its structural parameters, which is expressed by the following:

$$\sigma_c = \frac{105\pi E_0}{16}\left(\frac{d}{l}\right)^5_{eff} \varepsilon_c \tag{1}$$

where ε_c is the compression strain; E_0 is the carbon fibers elastic modulus in the longitudinal direction (E_0 = 230 GPa, [31]); σ_c is the compression stress (MPa); l is the inter-fiber length within one layer (m) and d is the uniformed carbon fiber's diameter (m) as shown in Fig. 2.

Based on Norouzifard's model, Gigos et al. [19] made some assumptions to simplify the GDL's compressive analytical model. Assumption 1 is explained in Fig. 2, it was observed that the real GDL was composed of carbon fibers randomly overlapped crossing. Obviously, within one layer, there were many quadrilaterals that could be idealized as some squares by carbon fiber decussations. Thus, the area of the small square or pore A_{pore}, as shown in Fig. 2, can be calculated by (2).

$$A_{pore} = (l-d)^2 \tag{2}$$

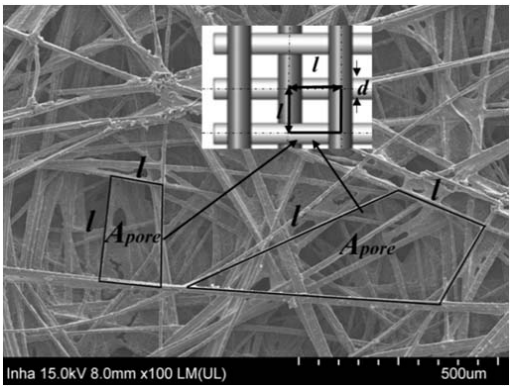

Fig. 2 A microstructure image of a commercial GDL

Assumption (2) was related to the GDL's porosity. The initial porosity of the GDL p_0, is generally defined as follows:

$$p_0 = \frac{V_{void}}{V_{total}} \approx \frac{A_{pore}}{A_{total}} \approx \frac{(l-d)^2}{l^2} \tag{3}$$

$$\frac{d}{l} \approx 1-\sqrt{p_0} \tag{4}$$

where V_{void} is the GDL's void volume (m^3); V_{total} is the GDL's total volume (m^3); A_{total} is the GDL's total surface area (m^2). However, during the compression test, the real porosity of the GDL decreases as the compressive load increases [32]. The real porosity of the GDL p during compression can be explained by follows:

$$1-\varepsilon_c = \frac{1-p_0}{1-p} \tag{5}$$

$$p = \frac{p_0-\varepsilon_c}{1-\varepsilon_c} \tag{6}$$

As a result, the simplified GDL's compressive analytical model can be expressed by (7).

$$\sigma_c = \frac{105\pi E_0}{16}\left(1-\sqrt{\frac{p_0-\varepsilon_c}{1-\varepsilon_c}}\right)^5 \varepsilon_c \tag{7}$$

However, if the above assumptions were elaborated, the analytical compressive model could be improved with higher accuracy. Based on these assumptions, this paper developed the GDL's compressive analytical model. In (3), the expression of initial porosity of the GDL p_0 by fiber's length l and diameter d is so rough that a dimensionless calibration parameter A (A ≥ 1) can be employed to calibrate, which is shown as follows:

$$\frac{d}{l} = A-\sqrt{p} \tag{8}$$

Hence, the GDL compressive analytical model can be modified as follows:

$$\sigma_c = \frac{105\mu\pi E_0}{16}\left(A-\sqrt{\frac{p_0-\varepsilon_c}{1-\varepsilon_c}}\right)^5 \varepsilon_c \tag{9}$$

where μ is a dimensionless calibration parameter which stands the structural differences between a real GDL and its compressive analytical model. Then, the GDL's compression modulus E can be calculated as:

$$E = \frac{d\sigma_c}{d\varepsilon} = \frac{105\pi\mu E_0}{16}\left(A-\sqrt{\frac{p_0-\varepsilon_c}{1-\varepsilon_c}}\right)^5 - \frac{525\pi\mu E_0\varepsilon_c}{32}\cdot \left(A-\sqrt{\frac{p_0-\varepsilon_c}{1-\varepsilon_c}}\right)^4 \cdot \sqrt{\frac{1-\varepsilon_c}{p_0-\varepsilon_c}}\cdot\frac{p_0-1}{(1-\varepsilon_c)^2} \tag{10}$$

B. In-plane Tension Numerical Model

From the in-plane tension test results, it is proved that the relationship between the GDL's tension strain ε_T and stress σ_T is nearly linear and it can be typically described by:

$$\sigma_T = k_T \cdot \varepsilon_T \tag{11}$$

where k_T is the in-plane tension modulus of the GDL (MPa).

C. Shear Numerical Model

According to our GDL's shear experimental results, its shear strain γ and stress τ can be expressed by:

$$\tau = \frac{k_c \cdot \Delta l}{A_{shear}} \tan\gamma \tag{12}$$

where k_c is the slope of GDL's force and deformation curves in shear tests (N/mm); A_{shear} is the cross section area (mm^2); Δl is the jig gap (mm). Thus, the shear modulus of the GDL G is calculated as:

$$G = \frac{d\tau}{d\gamma} = \frac{k_c \cdot \Delta l}{A_{shear}} \cdot \frac{1}{(\cos\gamma)^2} \tag{13}$$

III. Simulation

A. GDL's Stiffness Matrix Building

All the above models such as compression, tension, and shear numerical models were employed to build the stiffness matrix of the commercial GDL. Then, the stiffness matrix was implemented into the user-defined material model (UMAT) subroutine part of ABAQUS to do the simulation. In this investigation, GDL's material property parameters, in the constitutive equations of the stiffness matrix, were Young's modulus (E_x, E_y, and E_z), Poisson's ratios (ν_{yz}, ν_{zx}, and ν_{xy}), and shear modulus (G_{yz}, G_{zx}, and G_{xy}). Note that, for orthotropic materials, there are no coupling effects between the normal stresses (σ_{xx}, σ_{yy}, and σ_{zz}) and the shear strains (ε_{yz}, ε_{zx}, and ε_{xy}). Thus, according to Hook's law, the compliance matrix of the orthotropic materials can be described as:

$$\begin{bmatrix}\varepsilon_{xx}\\ \varepsilon_{yy}\\ \varepsilon_{zz}\\ \varepsilon_{yz}\\ \varepsilon_{zx}\\ \varepsilon_{xy}\end{bmatrix} = \begin{bmatrix} \frac{1}{E_x} & -\frac{\nu_{yx}}{E_y} & -\frac{\nu_{zx}}{E_z} & 0 & 0 & 0\\ -\frac{\nu_{xy}}{E_x} & \frac{1}{E_y} & -\frac{\nu_{zy}}{E_z} & 0 & 0 & 0\\ -\frac{\nu_{xz}}{E_x} & -\frac{\nu_{yz}}{E_y} & \frac{1}{E_z} & 0 & 0 & 0\\ 0 & 0 & 0 & \frac{1}{2G_{yz}} & 0 & 0\\ 0 & 0 & 0 & 0 & \frac{1}{2G_{zx}} & 0\\ 0 & 0 & 0 & 0 & 0 & \frac{1}{2G_{xy}} \end{bmatrix} \begin{bmatrix}\sigma_{xx}\\ \sigma_{yy}\\ \sigma_{zz}\\ \sigma_{yz}\\ \sigma_{zx}\\ \sigma_{xy}\end{bmatrix} \tag{14}$$

In (14), the given coefficients such as Young's modulus and Poisson's ratios have the relationships as:

$$\frac{\nu_{yz}}{E_y} = \frac{\nu_{zy}}{E_z},\ \frac{\nu_{zx}}{E_z} = \frac{\nu_{xz}}{E_x},\ \frac{\nu_{xy}}{E_x} = \frac{\nu_{yx}}{E_y} \tag{15}$$

After the inverse transformation of (14), the stiffness matrix can be explained by follows:

$$\begin{bmatrix}\sigma_{xx}\\ \sigma_{yy}\\ \sigma_{zz}\\ \sigma_{yz}\\ \sigma_{zx}\\ \sigma_{xy}\end{bmatrix} = \begin{bmatrix} \frac{1-\nu_{yz}\nu_{zy}}{E_yE_z\Delta} & \frac{\nu_{yx}+\nu_{zx}\nu_{yz}}{E_yE_z\Delta} & \frac{\nu_{zx}+\nu_{yx}\nu_{zy}}{E_yE_z\Delta} & 0 & 0 & 0\\ \frac{\nu_{xy}+\nu_{xz}\nu_{zy}}{E_zE_x\Delta} & \frac{1-\nu_{zx}\nu_{xz}}{E_zE_x\Delta} & \frac{\nu_{zy}+\nu_{zx}\nu_{xy}}{E_zE_x\Delta} & 0 & 0 & 0\\ \frac{\nu_{xz}+\nu_{xy}\nu_{yz}}{E_xE_y\Delta} & \frac{\nu_{yz}+\nu_{xz}\nu_{yx}}{E_xE_y\Delta} & \frac{1-\nu_{xy}\nu_{yx}}{E_xE_y\Delta} & 0 & 0 & 0\\ 0 & 0 & 0 & 2G_{yz} & 0 & 0\\ 0 & 0 & 0 & 0 & 2G_{zx} & 0\\ 0 & 0 & 0 & 0 & 0 & 2G_{xy} \end{bmatrix} \begin{bmatrix}\varepsilon_{xx}\\ \varepsilon_{yy}\\ \varepsilon_{zz}\\ \varepsilon_{yz}\\ \varepsilon_{zx}\\ \varepsilon_{xy}\end{bmatrix} \tag{16}$$

where $\Delta = \frac{1-\nu_{xy}\nu_{yx}-\nu_{yz}\nu_{zy}-\nu_{zx}\nu_{xz}-2\nu_{xy}\nu_{yz}\nu_{zx}}{E_xE_yE_z}$.

In this paper, due to GDL's porosity structures, its Poisson's ratios are zero [27], [33] (it means that $\nu_{yz}=\nu_{zy}=\nu_{zx}=\nu_{xz}=\nu_{xy}=\nu_{yx}=0$). Thus, $\Delta = \frac{1}{E_xE_yE_z}$. Hence, (16) can be simplified as follows:

$$\begin{bmatrix}\sigma_{xx}\\ \sigma_{yy}\\ \sigma_{zz}\\ \tau_{yz}\\ \tau_{zx}\\ \tau_{xy}\end{bmatrix} = \begin{bmatrix} E_x & 0 & 0 & 0 & 0 & 0\\ 0 & E_y & 0 & 0 & 0 & 0\\ 0 & 0 & E_z & 0 & 0 & 0\\ 0 & 0 & 0 & G_{yz} & 0 & 0\\ 0 & 0 & 0 & 0 & G_{zx} & 0\\ 0 & 0 & 0 & 0 & 0 & G_{xy} \end{bmatrix} \begin{bmatrix}\varepsilon_{xx}\\ \varepsilon_{yy}\\ \varepsilon_{zz}\\ \gamma_{yz}\\ \gamma_{zx}\\ \gamma_{xy}\end{bmatrix} \tag{17}$$

where, σ_{xx}, σ_{yy}, E_x, E_y, ε_{xx}, and ε_{yy} are the tension stress, tension modulus and tension strain in X direction Y direction, respectively; σ_{zz}, E_z, and ε_{zz} are the compression stress, compression modulus and compression strain in Z direction; G_{yz}, G_{zx}, G_{xy}, γ_{yz}, γ_{zx}, and γ_{xy} are shear stress and shear strain in YZ plane, ZX plane, and XY plane, respectively.

In the compression condition, according to (10), GDL's compression modulus can be calculated as:

$$E_z = \frac{105\pi\mu E_0}{16}\left(A-\sqrt{\frac{p_0-\varepsilon_{zz}}{1-\varepsilon_{zz}}}\right)^5 - \frac{525\pi\mu E_0\varepsilon_{zz}}{32}\cdot \left(A-\sqrt{\frac{p_0-\varepsilon_{zz}}{1-\varepsilon_{zz}}}\right)^4 \cdot \sqrt{\frac{1-\varepsilon_{zz}}{p_0-\varepsilon_{zz}}}\cdot\frac{p_0-1}{(1-\varepsilon_{zz})^2} \tag{18}$$

In the tension condition, it can be directly achieved that the in-plane Young's moduli of the GDL are expressed by:

$$\begin{cases} E_x = k_x \\ E_y = k_y \end{cases} \tag{19}$$

where k_x and k_y are the elastic modulus in X and Y directions for tension test, respectively.

In the shear condition, it can be observed from the stiffness matrix in (17) that

$$\begin{cases} \tau_{yz} = G_{yz} \cdot \gamma_{yz} \\ \tau_{xz} = G_{xz} \cdot \gamma_{xz} \\ \tau_{xy} = G_{xy} \cdot \gamma_{xy} \end{cases} \tag{20}$$

Based on the GDL's shear numerical model, the shear moduli are described in (13). For recognizing the shear modulus easily, we defined:

$$C\_G = \frac{k_c \cdot \Delta l}{A_{shear}} \tag{21}$$

where C_G is a constant. In this paper, what is noteworthy is that we just conducted shear test in the YZ plane and the XZ plane, without measuring the GDL's shear modulus in the XY plane. The value of the GDL's shear modulus in the XY plane, used for simulation, is in [34].

$$G_{yz} = C\_G_{yz} \frac{1}{(\cos \gamma_{yz})^2} \tag{22}$$

$$G_{xz} = C\_G_{xz} \frac{1}{(\cos \gamma_{xz})^2} \tag{23}$$

B. UMAT Coding

If we cannot find a suitable model in ABAQUS for materials' simulation, the part of user subroutines which could provide extremely powerful and flexible tools [35], [36] for user-defined materials is our best selection. UMAT can define the material constitutive model by describing its material Jacobian matrix (or stiffness matrix), to expend the ABAQUS functions. In general, UMAT can be almost used for the mechanical behavior analysis of any materials. To ensure UMAT implement successfully, it is typically written in FORTRAN. Significantly, one or more user subroutines must be included in one model through an ABAQUS execution command line option.

Fig. 3 illustrates the flow chart of the GDL's UMAT. There is a key step for the GDL's UMAT implementation, which is to input the material parameters into the comprehensive 3D constitutive model. These parameters of the GDL stand its material mechanical characteristics.

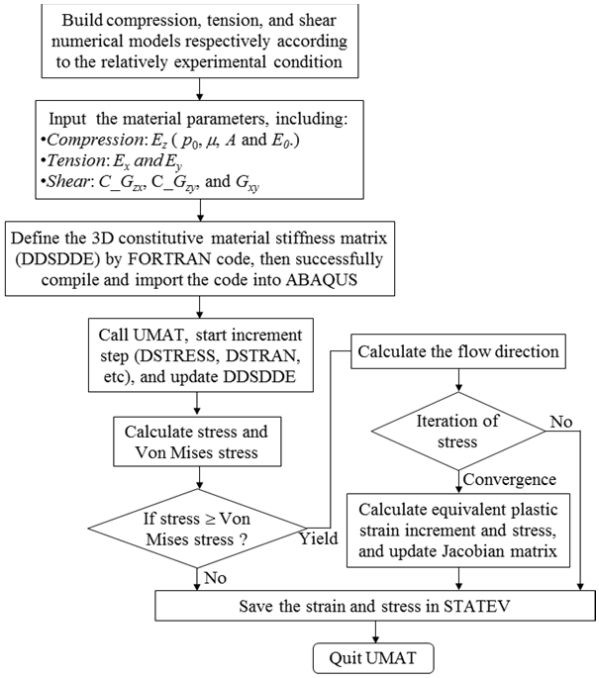

Fig. 3 The GDL's UMAT implementation flow chart

IV. Results and Discussion

With the aim of validating the GDL's comprehensive 3D nonlinear constitutive model, its numerical models were coded and implemented into the UMAT part of ABAQUS for simulation. Then, the simulation results were used for being compared with experimental data. The compression, in-plane tension and shear mechanical characteristics of the commercial GDL, included in experimental data and simulation results, were described in Figs. 4-6, respectively.

In Fig. 4, it can be concluded that the GDL shows obviously nonlinear compressive characteristics in its thickness direction by experimental data as well as the simulation results. Norouzifard [30] developed a novel analytical through-plane model of a GDL, where the GDL's microstructural characteristics and mechanical properties are included in. However, the model predicted that the GDL's compression behavior is linear within the compressive pressure larger than 1 MPa. Based on Norouzifard's accomplishments, Gigos et al. [19] made some assumptions to optimize and simplify the GDL's compressive analytical model that is used for the GDL's periodical compression analysis, and the theoretical stress versus strain curves from the analytical model show a good agreement with experimental data in cyclic loads processes. Even though Norouzifard and Gigos developed the GDL's compressive analytical model, both of their models were not implemented in any engineering software for simulation. This study not only improves the compressive model but also employs it into ABAQUS with the developed GDL's constitutive model for simulation, which could intuitively observe the GDL's deformation during simulation and accurately predict the GDL's mechanical behavior. And the

GDL's compressive model, as a subpart, could be also directly applied in a whole fuel cell's mechanical simulation.

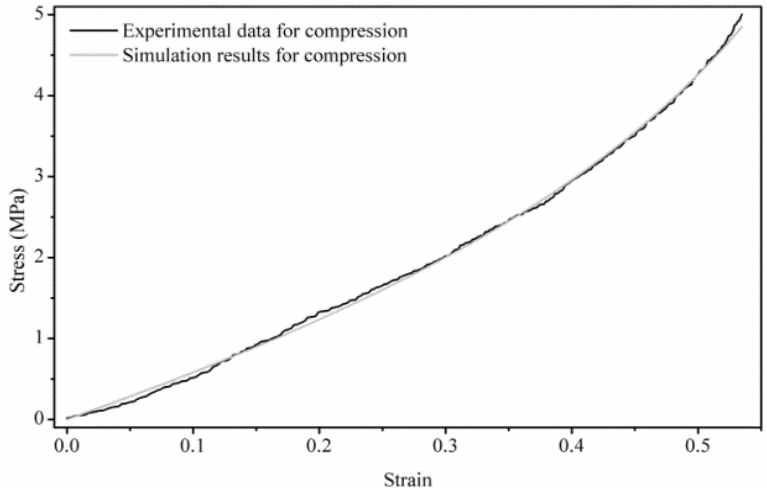

Fig. 4 Experiment and simulation stress vs. strain curves of the GDL in compression test

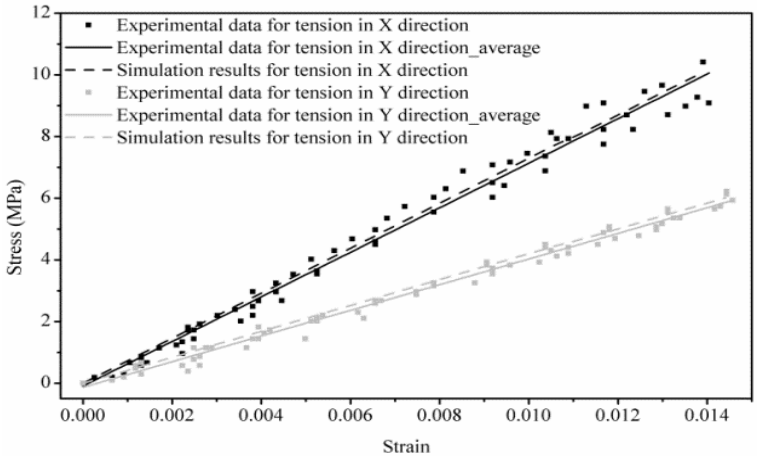

Fig. 5 Experiment and simulation stress vs. strain curves of the GDL in tension test

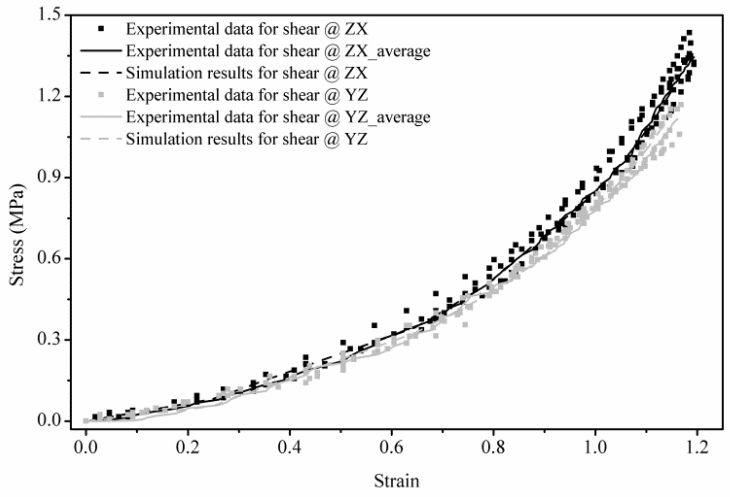

Fig. 6 Experiment and simulation stress vs. strain curves of the GDL in shear test

Fig. 5 describes the in-plane tension mechanical characteristics of the GDL by experiment and simulation results. It is found that the GDL shows greatly anisotropic and linear properties for its in-plane tension performance. Some researchers studied GDLs' in-plane mechanical characteristics by experimental methods [27], [33] without any simulation descriptions. This paper not only conducts the in-plane tension test but also builds the numerical model to analyze its behavior. Meanwhile, the simulation results from the numerical model are compared with the experimental data. As a result, they are in good accordance with each other.

Studies of GDL's shear performance are quite few. Some researchers predicted GDL's shear behavior, roughly [33], [37]. However, they lack compelling experimental data to confirm their accomplishments. This paper presents the shear mechanical characteristics of the GDL by experimental data as well as simulation results, as shown in Fig. 6. It is observed that the GDL's shear performance displays strongly nonlinear characteristics and slightly anisotropy. In addition, the simulation results from the shear numerical model are consistent with the experimental data.

In conclusion, all simulation results from the comprehensive 3D constitutive model of the GDL fit the experimental data quite well. Table I shows the related coefficients of determination for the simulation and experimental data.

TABLE I
COEFFICIENTS OF DETERMINATION FOR DIFFERENT MECHANICAL TEST

Test	Directions	Coefficients of determination
Compression	Thickness, or Z	0.9941
Tension	X	0.9912
	Y	0.9884
Shear	ZX plane	0.9893
	ZY plane	0.9925

V. CONCLUSIONS

In this investigation, a comprehensive 3D nonlinear constitutive model was developed to describe the GDL's mechanical behavior. In the comprehensive constitutive model, the GDL's microstructure characteristics and mechanical property parameters, such as carbon fiber's elastic modulus, porosity, in-plane elastic moduli, shear moduli, and Poisson's ratio, were included in. Then, the comprehensive constitutive model was coded and implemented in the UMAT of ABAQUS to verify its reliability. Thus, compression strain-stress, in-plane tensile strain-stress, and shear strain-stress curves of the GDL were shown by experimental data and simulation results, respectively. It is found that the experimental data, as well as the simulation results show a good agreement with each other, which indicates that the comprehensive 3D nonlinear constitutive model is with high reliability.

Furthermore, the constitutive model could be used for the GDL's mechanical analysis to as well as being embedded into a whole fuel cell model directly for simulation. With the help of computer simulation method, the GDL's mechanical deformation can be intuitively observed and analyzed. This research provides guidelines and views for the GDL's optimized manufacturing and application.

ACKNOWLEDGMENT

This research was supported by Inha University.

REFERENCES

[1] J-H. Wee, "Applications of proton exchange membrane fuel cell systems," *Renewable and sustainable energy reviews*, vol. 11, pp. 1720-1738, October 2007.
[2] X. Lü, Y. Qu, Y. Wang, C. Qin, and G. Liu, "A comprehensive review on hybrid power system for PEMFC-HEV: Issues and strategies," *Energ Convers Manage*, vol. 171, pp. 1273-1291, September 2018.
[3] R. K. A. Rasheed, Q. Liao, Z. Caizhi, and S. H. Chan, "A review on modelling of high temperature proton exchange membrane fuel cells (HT-PEMFCs)," *Int J Hydrogen Energ*, vol. 42, pp. 3142-3165, February 2017.
[4] V. Mehta and J. S. Cooper, "Review and analysis of PEM fuel cell design and manufacturing," *J Power Sources*, vol. 114, pp. 32-53, February 2003.
[5] D. Liu, L. Peng, and X. Lai, "Effect of dimensional error of metallic bipolar plate on the GDL pressure distribution in the PEM fuel cell," *Int J Hydrogen Energ*, vol. 34, pp. 990-997, January 2009.
[6] D. Qiu, P. Yi, L. Peng, and X. Lai, "Study on shape error effect of metallic bipolar plate on the GDL contact pressure distribution in proton exchange membrane fuel cell," *Int J Hydrogen Energ*, vol. 38, pp. 6762-6772, May 2013.
[7] P. Chippar, K. O, K. Kang, and H. Ju, "A numerical investigation of the effects of GDL compression and intrusion in polymer electrolyte fuel cells (PEFCs)," *Int J Hydrogen Energ*, vol. 37, pp. 6326-6338, April 2012.
[8] A. El-kharouf, T. J. Mason, D. J. L Brett, and B. G. Pollet, "Ex-situ characterisation of gas diffusion layers for proton exchange membrane fuel cells". *J Power Sources*, vol. 218, pp. 393-404, November 2012.
[9] J. A. Pelaez and S. G. Kandlikar, "Effects of Freezing and Thawing on the Structures of Porous Gas Diffusion Media", in *ASME 2007 5th International Conference on Nanochannels, Microchannels, and Minichannels*, Puela, 2007, pp. 401-408.
[10] D. Jones, "International Conference on Progress in MEA Materials for Medium and High Temperature Polymer Electrolyte Fuel Cells," *Fuel Cells*, vol. 11, pp. 714-714, December, 2011.
[11] A. Arvay, E. Yli-Rantala, C. H. Liu, *et al*, "Characterization techniques for gas diffusion layers for proton exchange membrane fuel cells – A review," *J Power Sources*, vol. 213, pp. 317-337, September 2012.
[12] L. Cindrella, A. M. Kannan, J. F. Lin, *et al*, "Gas diffusion layer for proton exchange membrane fuel cells—A review," *J Power Sources*, vol. 194, pp. 146-160, October 2009.
[13] D. M. Fadzillah, M. I. Rosli, M. Z. M. Talib, S. K. Kamarudin, and W. R. W. Daud, "Review on microstructure modelling of a gas diffusion layer for proton exchange membrane fuel cells," *Renewable and sustainable energy reviews*, vol. 77, pp. 1001-1009, September 2017.
[14] F. Lapicque, M. Belhadj, C. Bonnet, J. Pauchet, and Y. Thomas, "A critical review on gas diffusion micro and macroporous layers degradations for improved membrane fuel cell durability," *J Power Sources*, vol. 336, pp. 40-53, December 2016.
[15] R. Omrani and B. Shabani, "Gas diffusion layer modifications and treatments for improving the performance of proton exchange membrane fuel cells and electrolysers: A review," *Int J Hydrogen Energ*, vol. 42, pp. 28515-28536, November 2017.
[16] J. Park, H. Oh, T. Ha, Y. I. Lee, and K. Min, "A review of the gas diffusion layer in proton exchange membrane fuel cells: Durability and degradation," *Appl Energ*, vol. 155, pp. 866-880, October 2015.
[17] S. Park, J-W Lee, and B. N. Popov, "A review of gas diffusion layer in PEM fuel cells: Materials and designs," *Int J Hydrogen Energ*, vol. 37, pp. 5850-5865, April 2012.
[18] S. R. Dhanushkodi, F. Capitanio, T. Biggs, and W. Mérida, "Understanding flexural, mechanical and physico-chemical properties of gas diffusion layers for polymer membrane fuel cell and electrolyzer systems," *Int J Hydrogen Energ*, vol. 40, pp. 16846-16859, December 2015.
[19] P. A. Gigos, Y. Faydi, and Y. Meyer, "Mechanical characterization and analytical modeling of gas diffusion layers under cyclic compression," *Int J Hydrogen Energ*, vol. 40, pp. 5958-5965, May 2015.

[20] T. J. Mason, J. Millichamp, T. P. Neville, A. El-kharouf, B. G. Pollet, and D. J. L. Brett, "Effect of clamping pressure on ohmic resistance and compression of gas diffusion layers for polymer electrolyte fuel cells," *J Power Sources*, vol. 219, pp. 52-59, December 2012.
[21] V. Radhakrishnan and P. Haridoss, "Effect of cyclic compression on structure and properties of a Gas Diffusion Layer used in PEM fuel cells," *Int J Hydrogen Energ*, vol. 35, pp. 11107-11118, October 2010.
[22] V. Radhakrishnan and P. Haridoss, "Effect of GDL compression on pressure drop and pressure distribution in PEMFC flow field," *Int J Hydrogen Energ*, vol. 36, pp. 14823-14828, November 2011.
[23] Z. Y. Su, C. T. Liu, H. P. Chang, C. H. Li, K. J. Huang, and P. C. Sui, "A numerical investigation of the effects of compression force on PEM fuel cell performance," *J Power Sources*, vol. 183, pp. 182-192, August 2008.
[24] P. Zhou and C. W. Wu, "Numerical study on the compression effect of gas diffusion layer on PEMFC performance," *J Power Sources*, vol. 170, pp. 93-100, June 2007.
[25] V. Mishra, F. Yang, and R. Pitchumani, "Measurement and Prediction of Electrical Contact Resistance Between Gas Diffusion Layers and Bipolar Plate for Applications to PEM Fuel Cells," *J Fuel Cell Sci Tech*, vol. 1, pp. 2-9, March 2004.
[26] M. F. Serincan and U. Pasaogullari, "Effect of gas diffusion layer anisotropy on mechanical stresses in a polymer electrolyte membrane," *J Power Sources*, vol. 196, pp. 1314-1320, February 2011.
[27] P. A. García-Salaberri, M. Vera, and R. Zaera, "Nonlinear orthotropic model of the inhomogeneous assembly compression of PEM fuel cell gas diffusion layers," *Int J Hydrogen Energ*, vol. 36, pp. 11856-11870, September 2011.
[28] S. Li, J. Yuan, M. Andersson, G. Xie, and B. Sundén, "Influence of anisotropic gas diffusion layers on transport phenomena in a proton exchange membrane fuel cell," *International Journal of Energy Research*, vol. 41, pp. 2034-2050, May 2017.
[29] A. H. Mahmoudi, A. Ramiar, and Q. Esmaili, "Effect of inhomogeneous compression of gas diffusion layer on the performance of PEMFC with interdigitated flow field," *Energ Convers Manage*, vol. 110, pp. 78-89, February 2016.
[30] V. Norouzifard and M. Bahrami, "Deformation of PEM fuel cell gas diffusion layers under compressive loading: An analytical approach," *J Power Sources*, vol. 264, pp. 92-99, October 2014.
[31] D. Roylance, "Laminated composite plates", Massachusetts Institute of Technology CAMBRIDGE, Cambridge Mass, 2000.
[32] N. Khajeh-Hosseini-Dalasm, T. Sasabe, T. Tokumasu, and U. Pasaogullari, "Effects of polytetrafluoroethylene treatment and compression on gas diffusion layer microstructure using high-resolution X-ray computed tomography," *J Power Sources*, vol. 266, pp. 213-221, November 2014.
[33] J. Kleemann, F. Finsterwalder, and W. Tillmetz," Characterisation of mechanical behaviour and coupled electrical properties of polymer electrolyte membrane fuel cell gas diffusion layers," *J Power Sources*, vol. 190, pp. 92-102, May 2009.
[34] K. K. Poornesh, Y-J Sohn, G-G Park, and Yang T-H, "Gas-diffusion layer's structural anisotropy induced localized instability of nafion membrane in polymer electrolyte fuel cell," *Int J Hydrogen Energ*, vol. 37, pp. 15339-15349, October 2012.
[35] X. Peng and J. Cao, "A dual homogenization and finite element approach for material characterization of textile composites," Composites Part B: Engineering, vol. 33, pp. 45-56, January 2002.
[36] J. Zhang, N. Kikuchi, V. Li, A. Yee, and G. Nusholtz, "Constitutive modeling of polymeric foam material subjected to dynamic crash loading," *International Journal of Impact Engineering*, vol. 21, pp. 369-86, May 1998.
[37] K. K. Poornesh, C. Cho, and A. M. Rego, "Anisotropic Distribution of Elastic Constants in Fuel Cell Gas Diffusion Layers: Experimental Validation," *Energy and Power*, vol. 5, pp. 40-45, 2015.